A Low Computational Cost, Prioritized, Multi-objective Optimization Procedure for Predictive Control Towards Cyber Physical Systems

Clara Ionescu[1,2], (Senior Member, IEEE), Ricardo Cajo[1,2,3], (Member, IEEE)
Shiquan Zhao[1,2,4], Mihaela Ghita[1,2], (Student Member, IEEE), Maria Ghita[1,2], (Student Member, IEEE), Dana Copot[1,2], (Member, IEEE)

[1]Dynamical Systems and Control Research Group, Department of Electromechanical, Systems and Metal Engineering, Ghent University, Ghent B-9052, Belgium
[2]EEDT Decision & Control, Flanders Make, Ghent B-9052, Belgium
[3]Escuela Superior Politécnica del Litoral ESPOL, Campus Gustavo Galindo km 30.5 Via Perimetral, P.O. Box 09-01-5863 Guayaquil, Ecuador
[4]College of Automation, Harbin Engineering University, Harbin 150001, China

Corresponding author: Clara Ionescu (e-mail: claramihaela.ionescu@ugent.be).

ABSTRACT Cyber physical systems consist of heterogeneous elements with multiple dynamic features. Consequently, multiple objectives in the optimality of the overall system may be relevant at various times or during certain context conditions. Low cost, efficient implementations of such multi-objective optimization procedures are necessary when dealing with complex systems with interactions. This work proposes a sequential implementation of a multi-objective optimization procedure suitable for industrial settings and cyber physical systems with strong interaction dynamics. The methodology is used in the context of an Extended Prediction self-adaptive Control (EPSAC) strategy with prioritized objectives. The analysis indicates that the proposed algorithm is significantly lighter in terms of computational time. The combination with an input-output formulation for predictive control makes these algorithms suitable for implementation with standardized process control units. Three simulation examples from different application fields indicate the relevance and feasibility of the proposed algorithm.

INDEX TERMS priority objectives, multi-objective optimization, model predictive control, steam power plant, unmanned aerial vehicle, drug regulatory network, interaction, safety.

I. INTRODUCTION

FROM recent reports on cyber-physical systems (CPS) such as [1], it follows that CPS have heterogeneous systems with heterogeneous signal types of interaction among them. Given their large scale and heterogeneity, the economic, performance, safety and other objectives are relevant at different levels of operation and are active at different time scales throughout the CPS operation. A common feature is that decoupling control is replaced by distributed control, as the interactions increase their relevance within the CPS performance. For instance, to develop a high-performance compensatory control system for vehicle power train, accurate estimations of the unmeasurable hybrid states, including discrete backlash nonlinearity and continuous half-shaft torque, are of great importance [2]. In addition, the safe operation of the electric vehicle is related with the braking system. Hence, an accurate estimation of brake pressure is very importance for the design and control of automotive CPS. In [3] a novel probabilistic estimation methods of brake pressure based on multilayer artificial neural networks (ANNs) with Levenberg-Marquardt backpropagation (LMBP) training algorithm is developed. This method shows a superiority in estimation accuracy of the brake pressure, with respect to other learning-based methods.

On the other hand, driving behaviors are closely related to fuel efficiency. The difference in fuel consumption between

normal and aggressive driving is estimated to be as high as 40% [4], [5]. As for challenges and opportunities, a key driver is the necessity of a multidisciplinary and an interdisciplinary approach to resolve such complex CPS. As given in [1], two of the most important CPS are biomedical and health-care systems and the next-generation of air transportation systems, both exemplified in this work. For all CPS, the following requirements prevail: i) large scale real time optimization algorithms; ii) multiple objective optimization; iii) automation with degradation modes (de-tuning); iv) safety and monitoring methods; v) distributed decision making; vi) data fusion from various sub-systems.

According to the latest reviews of industrially relevant control strategies, it follows that the most used in practice is Proportional-Integral-Derivative (PID) control followed by Model-based Predictive Control (MPC) [6]–[8]. Although easy to implement and accounting for 90% of the regulatory loops in any process, PID control has a serious drawback: it does not optimize the control action for apriori given constraints [9]. By contrast, MPC uses a cost function optimization which takes into account constraints while calculating the best input to the process given current conditions/operating point and future predicted process dynamics [10]–[14]. For accurate prediction and improved loop performance, MPC requires the availability of a good process model [15], [16]. Often, such a model is limited to a range of operating conditions, i.e. is a linear approximation of a nonlinear dynamic function. Additionally, the presence of interactions among various sub-systems of the global process need to be incorporated into the MPC formulation for satisfying the global performance specifications. In the context of complex CPS with interactions, fully multivariable MPC control is no longer feasible due to large scale and high complexity, while decentralized PID control leads to poor performance and possibly unstable situations [17]. From [1] it followed as natural solution was to use the potential of distributed MPC architectures as well suited alternatives for control of CPS [18]–[20]. Still, these formulations are far from being user-friendly as operator guide in an industrial setting, with non-control expert support. The support for plant operator in terms of tuning MPC algorithms has been available throughout decades from both academia and industry pioneers [15], [21]–[24], and recently successfully revisited on a manifold of simulated and experimental plants [25]. Complex industrial processes consist of interactions at various levels and coming from manifold sub-systems. Each sub-system plays its own role within a global convergence of the CPS to the desired product specifications. These specifications are dominated by the requirement for safety operation (which includes stability), within limit intervals for the manipulated variables and controlled outputs of the involved processes. When multi-objective optimization is required, there exist a manifold of academic solutions with stability guaranteed [26]–[29]. Some of them have also been applied to specific industrial settings, although their number remains limited [30]–[33]. Industry has already proposed and implemented process control unit tools for multi-objective optimization with priority constraint for model predictive control [31], [34].

In this paper we investigate the feasibility of a minimal model information multivariable process included in a multi-objective optimization scheme with prioritized objectives for the Extended Self-Adaptive Prediction Control (EPSAC). The originality of the proposed methodology is the low-computational cost implementation; i.e. the sequential priority evaluation in the algorithm and resuming the optimization at each sampling time with a single priority active at each time. The priority evaluation is based on past monitoring information available at each sampling time of loop execution. In the traditional MPC, the influence from constraints will always be considered to obtain the optimal inputs for the system. For example, the quadratic programming (QP) can be applied, which considers the constraints in each sampling time. However, there is not always setpoint changes or large scale of disturbances during the operation of the system, and most of time the system operates at a stable operating point with small scale of disturbances. During this kind of period, the only thing to be considered is energy, in which the control effort will always keep the same as the last sampling time. Hence, no optimization process exists, and there is a huge reduction in computing time. Our method keeps a minimal mathematical complexity as to allow ease of implementation in real-time process operation units like CPS, which are an integration of interconnections between cybernetic and physical subsystems through interfaces between software components and interaction of hardware components connected by wired or wireless communications [35], [36]. The specific input-output formulation of the model based predictive control used in this study allows to directly plug into the process variables. The physical processes studied here are three multivariable systems with significantly different dynamics, of which two are derived from listed relevant CPS applications [37]. A comparison between the fully optimized process performance and computational time is given against the proposed multi-objective prioritized optimization algorithm.

The paper is organized as follows. The proposed methodology is summarized in the next section, followed by a simulation analysis on three representative CPS (sub-)processes in section III. A discussion is given in the final section to pinpoint the main conclusions of this work.

sectionProposed Methodology

A. BASIC MPC INPUT-OUTPUT DATA FORMULATION

Among the many formulations of MPC methodologies, there is the EPSAC algorithm, developed in late 70s as operator guide [21], and initially conceived as an algorithm requiring minimal computational effort, given the available computational power at that time [38]. Hence, it has been successfully applied in industry, as summarized in [39]. Hitherto, it was applied in a manifold of technical and non-technical areas, while being recently introduced in the pharmaceutical indus-

try [40]. Stability and feasibility of this algorithm have been given in [41], [42] and robustness has been discussed in [43].

As most of the data available in industry has the form of input-output data, the MPC formulation investigated in this paper will consider to use such raw data [9]. This allows significant reduction in implementation complexity, since industrial instrumentation can handle such data format in standard setup conditions [44], [45]. The prediction model usually is an approximation as first-order plus dead time by the operator, or the result of a small amplitude sinusoidal test to obtain the frequency response slope in a given bandwidth of the process [9], [46]. Since the system is composed of multiple input and multiple output variables, these are apriori selected by the user according to their relevance in the physical production process. The models developed are a set of input-output functions characterizing the main process dynamics and the internal interactions in a minimal number of parameters. Measurable or predictable disturbances can be also incorporated using such input-output models [47], [48]. Next to model development, an uncertainty index can be defined to indicate how much trust the controller can have in the predicted future dynamics of the plant. This is then used in the real-time multi-objective optimization cost function (e.g. energy based, performance based, time-based, or combinations thereof) taking into account constraints and tuned for robustness as a function of this uncertainty degree [25]. Realignment procedures to fed back the true measured output of the process as opposed to only using the predicted output, allow for model adaptation during operation. This can be achieved using recursive identification algorithms, or correlation models on how the process dynamics change during variations in operating conditions.

The basic equation of EPSAC for a single-input single-output process is given by:

$$y(t) = x(t) + n(t) \tag{1}$$

where t is the discrete-time index (will be omitted in the remainder of the paper for simplicity of notation) and the output of the process $x(t)$ is predicted based on the past model output and past process inputs:

$$x(t) = f[x(t-1), x(t-2), ..., u(t-1), u(t-2), ...] \tag{2}$$

and a term $n(t)$ containing disturbances, noise and model mis-match. Notice that these functions depend on past inputs and past model outputs and may have any structure: linear, nonlinear, neural networks, etc. There exists also the variant where the past measured outputs of the process are used instead of past model outputs, and this is known as the realigned process model scheme; for details see [39].

The term in $n(t)$ denotes the disturbance and includes errors effects, modelled by coloured noise:

$$n(t) = \frac{C(q^{-1})}{D(q^{-1})} e(t) \tag{3}$$

with $e(t)$ white noise signal and q^{-1} the shift operator. The future response in linear MPC is the cumulative result of two effects:

$$y(t+k|t) = y_{base}(t+k|t) + y_{opt}(t+k|t) \tag{4}$$

where k is the sample index. The notation $(t+k|t)$ denotes here the future values, postulated at time t. The base response $y_{base}(t+k|t)$ can be calculated with the process and noise model for a generic control scenario u_{base}. For linear systems, the choice for these values is not important (superposition principle applies); for nonlinear systems, their choice is recommended as being the last input value to the process $u(t-1)$. The second component, y_{opt}, is the effect of optimizing the future control actions $\delta u(t|t), ..., \delta u(t + Nu - 1|t)$ defined as $\delta u(t+k|t) = u(t+k|t) - u_{base}(t+k|t)$, with $u(t+k|t)$ the optimal control input. The controller has N_c degrees of freedom, defined by the control horizon. The postulated optimal output can be calculated using the step response coefficients matrix G as defined in [39]. For linear, unconstrained systems, this matrix can be calculated only once from the process model and kept constant. However, in presence of (varying) constraints, nonlinear dynamics or varying process parameters, it is advisable to determine the content of G at every sampling time from the real process. The vector y_{opt} has the following matrix form:

$$
\begin{bmatrix}
y_{opt}(t+N_1|t) \\
y_{opt}(t+N_1+1|t) \\
... \\
... \\
y_{opt}(t+N_2|t)
\end{bmatrix}
=
\begin{bmatrix}
h_{N_1} & h_{N_1-1} & \cdots & g_{N_1-N_c+1} \\
h_{N_1+1} & h_{N_1} & \cdots & ... \\
... & ... & \cdots & ... \\
... & ... & \cdots & ... \\
h_{N_2} & h_{N_2-1} & \cdots & g_{N_2-N_c+1}
\end{bmatrix}
\begin{bmatrix}
\delta u(t|t) \\
\delta u(t+1|t) \\
... \\
\delta u(t+N_c-1|t)
\end{bmatrix}
\tag{5}
$$

In this equation, $y_{opt}(t+k|t)$ denotes the part in the predicted process output $y(t+k|t)$ coming from optimizing control action $\delta u(t+k|t)$. The matrix relating these two variables is the step response g and impulse response h coefficients, hence the G-matrix.

The cumulative response (4) of optimal and base response deliver the key equation for unconstrained EPSAC:

$$\mathbf{Y} = \bar{\mathbf{Y}} + \mathbf{G} \cdot \mathbf{U} \tag{6}$$

with $\mathbf{Y} = [y(t+N_1|t)...y(t+N_2|t)]^T$, $\mathbf{U} = [\delta u(t|t), ..., \delta u(t+N_c-1|t)]^T$, $\bar{\mathbf{Y}} = [y_{base}(t+N_1|t)...y_{base}(t+N_2|t)]^T$ and $\mathbf{G} \cdot \mathbf{U}$ calculated from (5); notice that this equation, in the special case of $N_c = 1$ reduces to a scalar and it delivers the explicit solution of the first step in the flowchart given in Fig. 1. In order to find the optimal part δu, the following cost functions are applied according to different working state:

If safety condition is not satisfied, the objective function for EPSAC is defined as:

$$
J = \sum_{k=N_1}^{N_2} [r(t+k|t) - y(t+k|t)]^2 + \lambda \sum_{k=0}^{N_c-1} [\delta u(t+k|t)]^2
$$
$$
\texttt{Subject to:} \quad u_{min} \le u(t) \le u_{max}
$$
$$
-y_{min} + \varepsilon \le y(t) \le y_{max} - \varepsilon
$$
$$\tag{7}$$

where, λ is the weighting factor, r is the reference to follow, N_1 and N_2 are the minimum and maximum prediction

horizons. In this case, the future control actions $u(t)$ can be obtained by minimizing the cost function given in (7).

If safety condition is satisfied, but the tracking error is out of tolerance intervals, the objective function for EPSAC is defined as:

$$J = \sum_{k=N_1}^{N_2} [r(t+k|t) - y(t+k|t)]^2 \qquad (8)$$

In this case no constraints are necessary. Therefore the optimal δu can be obtained with matrix calculation.

$$\mathbf{U}^* = [\mathbf{G^T G}]^{-1} \mathbf{G^T} [\mathbf{R} - \overline{\mathbf{Y}}] \qquad (9)$$

where, $\mathbf{U}^*$ is the optimal sequence of δu and $\mathbf{R} = [r(t + N_1|t)...r(t+N_2|t)]^T$.

If safety and tracking error conditions are both satisfied, the objective function for EPSAC is defined as:

$$J = \sum_{k=0}^{N_c-1} [\delta u(t+k|t)]^2 \qquad (10)$$

In this case no constraints are necessary and δu only needs to be kept as 0.

B. MULTI-OBJECTIVE OPTIMIZATION WITH PRIORITIES

At this point, everything is ready for the next step, i.e. the prioritized multi-objective optimization (MO) algorithm from Fig. 1. This is a simplified approach compared to those proposed in literature [28], [29], [33], [49]–[51]. MO algorithms with artificial intelligence data processing methods such as in [52], [53] can deal with great amount of data. By contrast, nonlinear functions can accommodate some of the exotic dynamics reducing the size of the problem but increasing numerical complexity in solving the MO problem [34]. Recent implementable solutions for existing infrastructure are possible in a portable environment [54].

Consider the MO flowchart depicted in Fig. 1. As with any process, the safety constraint is set as a hard constraint, given limit values intervals for all input-output variables it follows.

- check safety limit: is it fulfilled? when this condition is not satisfied, a pre-set of (suboptimal) safety values are given to the process operation units. This step is implemented as proposed in [31]. Consequently, the loop stops optimization and goes to the next sampling time;
- if the safety condition is fulfilled, then the next objective with next level priority is evaluated; i.e. if the output is within the tolerance intervals. If yes, then the optimization evaluates the next priority level, i.e. minimize control effort or energy.
- at every sampling time, the set of objectives are evaluated/executed in order of their priority;
- once an objective is optimized, the loop goes to the next sampling interval and repeats the procedure.

In the MOMPC, the safety is guaranteed by presenting the system variables are in the interval of the corresponding ranges, for example the upper bound and lower bound. The

tracking performance is indicated with the Integrate Relative Error. And the energy is indicated with the control effort. For example, in the steam/water loop the control efforts are about the opening of valves. Due to that the hydraulic cylinder is linked with the valve in the steam/water loop, the frequent changes in valves mean the frequent changes in hydraulic cylinder, which will result in a large amount of energy cost. In this sense, the energy will be saved if there is no change in the control effort.

The performance and effort are soft constraints, i.e. they are tailored to fit the objective at hand and not to minimize a specific cost goal. This allows a much faster computational convergence while process operation remains active within safety bounds. The sequential (prioritized) flowchart is iterated at every sampling period and the computational time within each iteration is recorded.

C. DEALING WITH DELAY AND NONLINEAR DYNAMICS

As the prediction step is in form of (6) and G-matrix can be time-variable, it implies flexibility to modeling or to uncertainty [25]. Such simple adaptation property to all types of model (linear or nonlinear processes) has been mentioned in a previous adaptive control work; suggesting that an instant input-output modeling with a variable gain can express all model dynamics and significantly reduce complexity in modeling [55], [56]. As long as adaptation gain is time invariant, i.e. not constant and updated at each iteration, it can express instant input-output relations of all real systems whether or not they are linear or not. This property was used in an adaptive gradient descent control method easy to implement and low-computational complexity [55], [56]. The study demonstrated that it works well for stable plant functions. In a similar manner we obtain the model flexibility by updating G-matrix at every sampling time instead of consideration of a constant G-matrix.

Hence, for nonlinear systems, linearization of the process model is not necessary, in the condition that the *G*-matrix is updated at every sampling time in relations (5)-(6). However, the step input applied to the real process to obtain this G-matrix coefficients requires an amplitude in the region of the expected steady state values of the controller output. If this is not the case, the information is not useful to the controller as due to nonlinear dynamics, if a large input value is used, then the *G* matrix has no longer information upon the specific operation point currently used. See further details in [39]. A schematic flowchart is given in the blue rectangle area denoted EPSAC in Fig. 3.

The complexity of the prediction procedure is increasing for systems with variable time delay than for those with constant time delay. This occurs frequently in CPS as part of the control over communication networks problem. For a system with time delay, changes in the controlled variable (i.e. in the output of the process) are only visible once the time delay has passed. Therefore, in order to find the optimal control sequence only output predictions occurring after the time delay should be taken in the cost function. This means
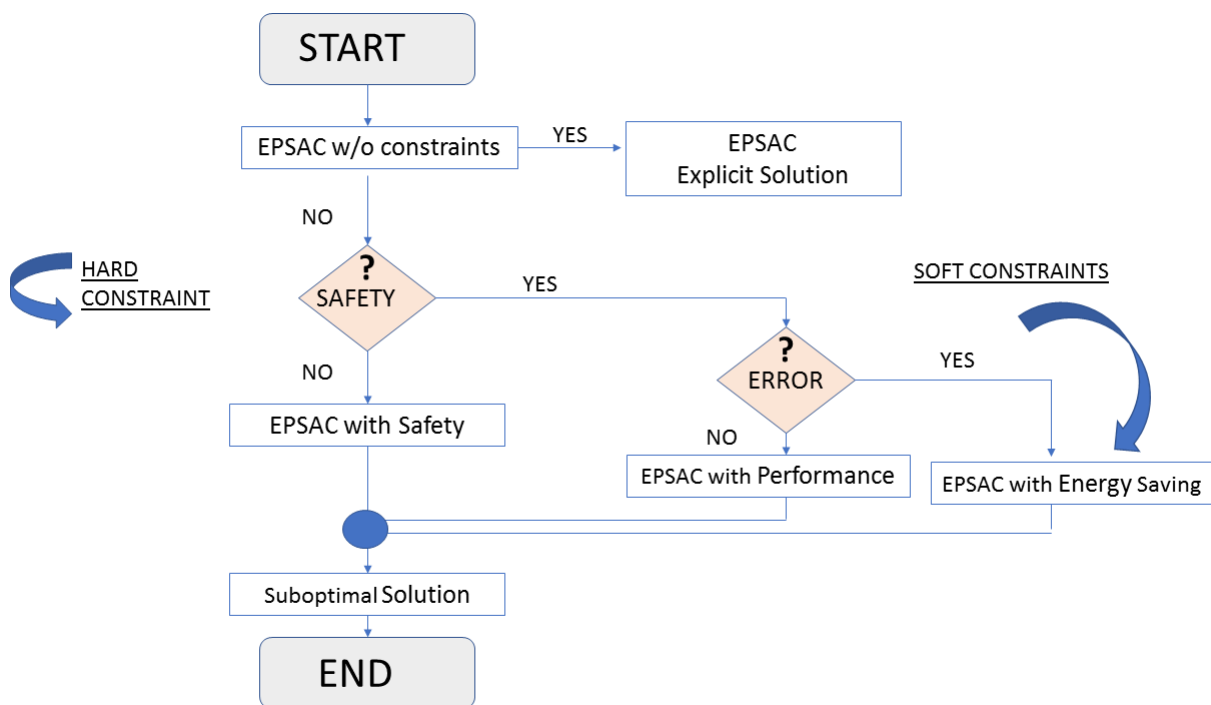
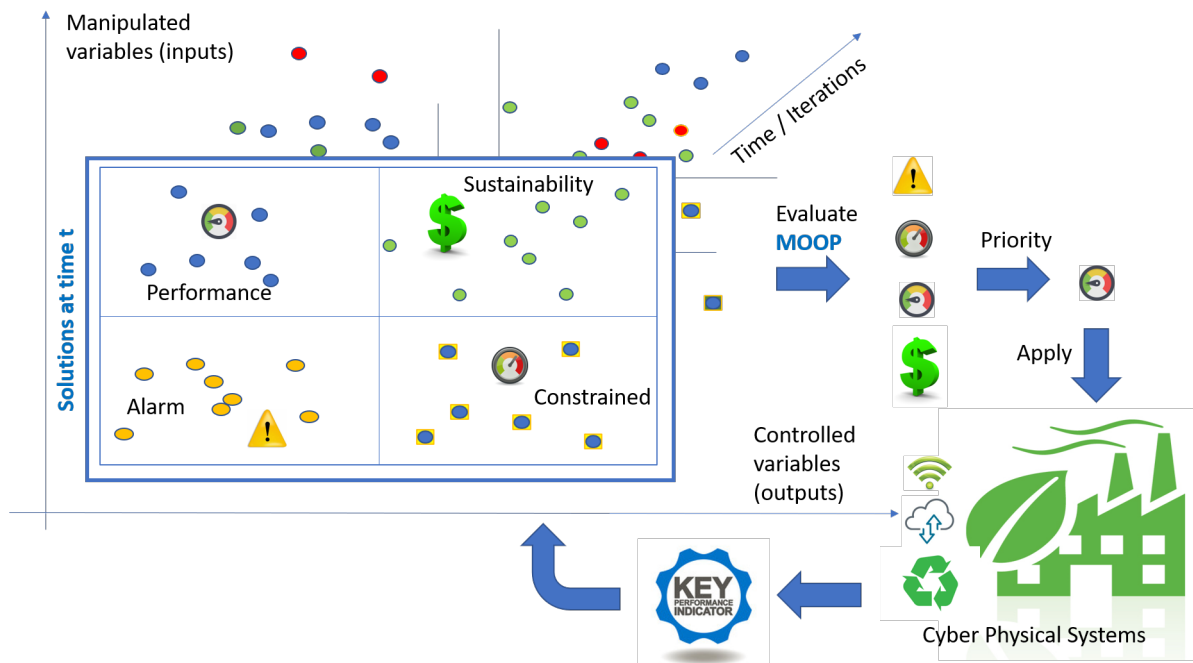FIGURE 1: Flowchart of the sequential prioritized optimization scheme

FIGURE 2: Graphical abstract of the optimization concept and methodology

that $N_1 = 1 + delay$. For systems with constant time delay this is easy to implement. Then the maximum prediction horizon N_2 can be set to an appropriate value that ensures a stable and robust response and the control loop can be operated with fixed controller parameters.

However, for systems with a variable time delay, such as those presented in [57]–[59], the values of N_1, N_2 and the size of the matrices used in the MPC formulation vary with the number of dead-time samples. To avoid increased matrix computation times and other implementation pitfalls, the structure of the process model is revised to design a predictive controller with constant design parameters. The generic principle valid for both SISO and MIMO processes is illustrated in Fig. 3 [58], [60], [61].

From figure 3, we can observe that at each sampling instant, the delay-free model output $x(t)$, resulting from the process dynamics only, is calculated using the stored values $[x(t-1), ..., u(t-1), ...]$. At the same sampling instant, the variable time delay is estimated/computed. Once the delay value in samples $delay = N_d$ is known, $x(t - N_d)$ can be selected out of the stored x-values, such that $z(t) = x(t - N_d)$. In this way, the prediction procedure is thoroughly simplified, resulting in a Smith predictor-like scheme, with separation of the delay-free part of the process and the varying time delay on the other hand. In such approach the minimum prediction horizon N_1 is no longer varying and is equal to one sample and all other optimization variables (matrices and vectors) containing this value no longer vary in size.

II. SIMULATION ANALYSIS

A. EXAMPLE 1: EMERGENCY DRONE PATH PLANNING

This example is a part of a larger system depicted in Fig. 4, i.e. emergency drone activation for emergency medicine [62], [63]. It follows the more generic concept of next-generation air transportation systems featured in [1]. The purpose is to bring the drone in a safe manner and through the shortest path to the location of a prospective victim (B) to assist in heart resuscitation before the ground ambulance arrives from its original location (A). As the system is extremely fast, low computational times of multi-objective optimization is a highly attractive feature.

Essentially, the drone is a multivariable and highly non-linear system with unstable open loop dynamic features [64]. However, due to the embedded attitude controller, it can be considered as a linear time invariant (LTI) system [65]. The linear models for each movement have been obtained using the prediction error method with a pseudo-random binary sequence (PRBS) excitation, as reported in [66], [67]. The over-simplified quadrotor model used for both simulation and prediction in the MPC scheme are:

$$\begin{cases} H_x(s) = \frac{x(s)}{V_{in}^x(s)} = \frac{7.27}{s(1.05s+1)}e^{-0.1s} \\ H_y(s) = \frac{y(s)}{V_{in}^y(s)} = \frac{7.27}{s(1.05s+1)}e^{-0.1s} \\ H_{altitude}(s) = \frac{z(s)}{V_{in}^z(s)} = \frac{0.72}{s(0.23s+1)}e^{-0.1s} \\ H_{yaw}(s) = \frac{\psi_{out}(s)}{V_{in}^\psi(s)} = \frac{2.94}{s(0.031s+1)}e^{-0.1s} \end{cases} \quad (11)$$

where $[x, y, z, \psi_{out}]$ are the system outputs for x, y, z positions (m) and *yaw* angle (rad). The system has four manipulated variables $[V_{in}^x, V_{in}^y, V_{in}^z, V_{in}^\psi]$ which correspond to linear velocity commands encoded under a specific protocol for the drone. These high-level control signals are normalized between $[-1, 1]$ and represent the percentages between $[0 - 100]\%$ of the configured values for the respective movements of the quadrotor. The controller parameters for MO-MPC and MPC are given in Table 1.

TABLE 1: Controller Parameters

Con-trol	N_1 Samples	N_2 Samples	N_c Samples	$T_s(s)$	Noise Filter:C/D
x,y	3	12	1		
z	3	12	1	0.066	$\frac{C(q^{-1})}{(1-q^{-1})A(q^{-1})}$
yaw	3	6	1		

The path followed by the AR.Drone during a certain task is shown in Fig. 5. The task consists in sequentially following the waypoints, starting at point 0 and ending at 6. On the other hand, the tracking control performance for the positions x, y, z and angle / orientation (yaw) of the quad-rotor are shown in Fig. 6 to Fig. 8.

Finally, the computational time, tracking error and disturbance rejection for both controllers with different control horizon values is shown in Fig. 9. It is important to emphasize that this plot was obtained during the path-follow between the points 0 to 1.

Fig. 9 indicates that the proposed method has a shorter computational time than the classical MPC approach, for all control horizon values. On the other hand, it is important to emphasize that the trade-off value between the computational time in favour of a better tracking error or disturbance rejection in the MPC requires a value of $5 < N_c < 6$. While, the MO-MPC this trade-off value is $1 < N_c < 2$, which indicates that the computational complexity of classical MPC is higher than the proposed MO-MPC for this system. The performance indexes are summarized in the Table 2, with definitions in (12). It can be observed a reduction of $10 - 25\%$ in the overall cost for the proposed MO-MPC algorithm.

$$\begin{cases} IAE_i = \sum_{k=0}^{N_s-1} |r_i(k) - y_i(k)| \;\; (i = 1, 2, \cdots, 4) \\ ISE_i = \sum_{k=0}^{N_s-1} (r_i(k) - y_i(k))^2 \;\; (i = 1, 2, \cdots, 4) \\ ISU_i = \sum_{k=0}^{N_s-1} (u_i(k) - u_{ssi}(k))^2 \;\; (i = 1, 2, \cdots, 4) \end{cases} \quad (12)$$

B. EXAMPLE 2: STEAM-WATER LOOP MANAGEMENT IN LARGE SHIPS

The second example is a highly complex system with high degree of interaction among the sub-systems (five). These sub-processes are common in chemical, pulp, paper, petro-chemical and steel industry. In this particular example, the
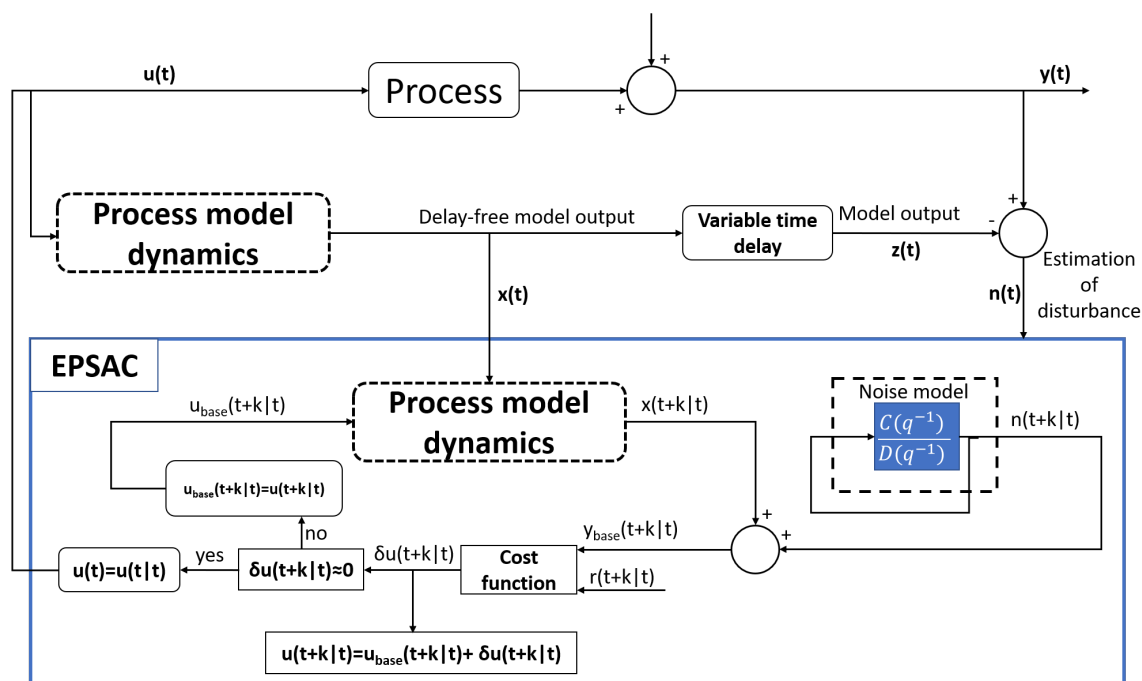
FIGURE 3: Smith-Predictor like EPSAC-MPC formulation for processes with variable time delays (SISO) or processes with multiple time delay functions (MIMO).

FIGURE 4: Conceptual representation of the emergency drone context for rescue assistance. This example is part of a more generic concept: next-generation air transportation systems.
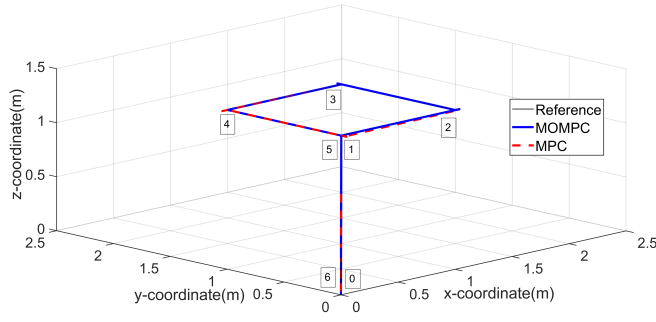
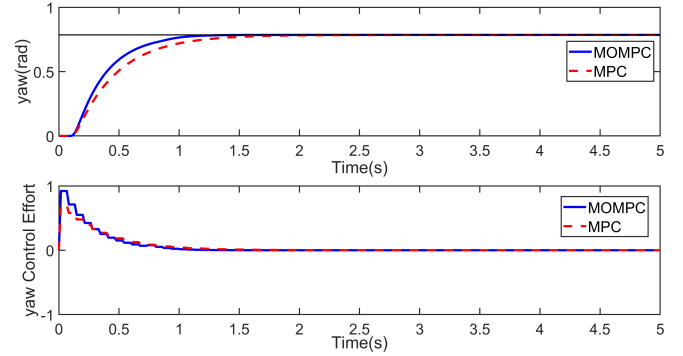FIGURE 5: 3D Trajectory tracking of the AR Drone system
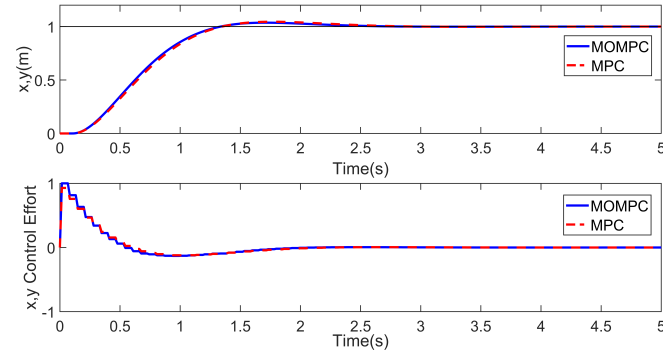

FIGURE 6: Trajectory tracking for *x*, *y* position
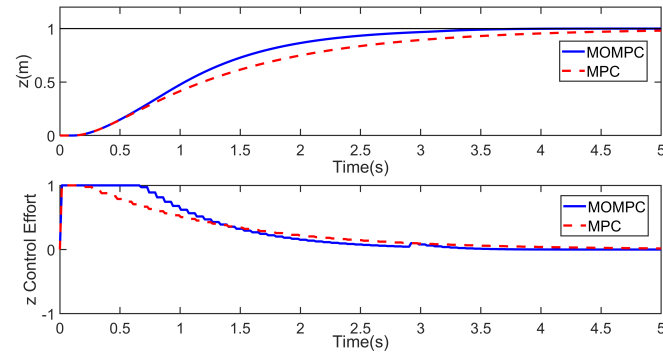

FIGURE 7: Trajectory tracking for *z* position

FIGURE 8: Trajectory tracking for *yaw* position

TABLE 2: Performance indexes for the controllers

Control	Index	MO-MPC	MPC
x	IAE	169.65	176.76
	ISU	42.27	37.96
	ISE	8.2237	9.08
y	IAE	167.65	174.76
	ISU	42.27	37.96
	ISE	2.94	3.27
z	IAE	146.29	185.72
	ISU	125.54	97.13
	ISE	2.12	3.13
yaw	IAE	18.84	23.45
	ISU	8.43	6.20
	ISE	1.95	2.60
Total	IAE	**125.60**	140.17
	ISU	**54.62**	44.81
	ISE	**3.81**	4.52

method is applied to a steam/water loop with five inputs and five outputs as detailed in [68] and depicted in Fig. 10. The system is highly nonlinear [69] but a simplified nominal model is given by the set of equations (13), in which the input vector $u = [u_1, u_2, u_3, u_4, u_5]$ contains the positions of the valves that control the flow rates of feedwater to the drum (u_1), exhaust steam from the exhaust manifold (u_2), exhaust steam to the deaerator (u_3), water from the deaerator (u_4) and water to the condenser (u_5); the output vector $y = [y_1, y_2, y_3, y_4, y_5]$ contains the values of the water level in drum (y_1), pressure in exhaust manifold (y_2), water level (y_3)

and pressure (y_4) in deaerator, and water level of condenser (y_5), respectively.

$$
\begin{bmatrix} y_1 \\ y_2 \\ \vdots \\ y_5 \end{bmatrix} \begin{bmatrix} G_{11} & G_{12} & \cdots & G_{15} \\ G_{21} & G_{22} & \cdots & G_{25} \\ \vdots & \vdots & \ddots & \vdots \\ G_{51} & G_{52} & \cdots & G_{55} \end{bmatrix} \begin{bmatrix} u_1 \\ u_2 \\ \vdots \\ u_5 \end{bmatrix} \quad (13)
$$

where:

$$G_{11}(s) = \frac{0.0000987}{(s+0.1131)(s+0.0085+0.032j)(s+0.0085-0.032j)}$$

$$G_{22}(s) = \frac{0.7254}{(s+1.2497)(s+0.0223)}$$

$$G_{23}(s) = \frac{-0.5}{(s+1.9747)(s+0.0253)}$$

$$G_{33}(s) = \frac{0.0132}{(s+0.0265+0.0244j)(s+0.0265-0.0244j)}$$

$$G_{34}(s) = \frac{-0.009}{(s+0.0997)(s+0.0411}$$

$$G_{41}(s) = \frac{-0.0008}{(s+0.012+0.126j)(s+0.012-0.126j)}$$

$$G_{44}(s) = \frac{0.0005152}{(s+0.012+0.038j)(s+0.012-0.038j)}$$

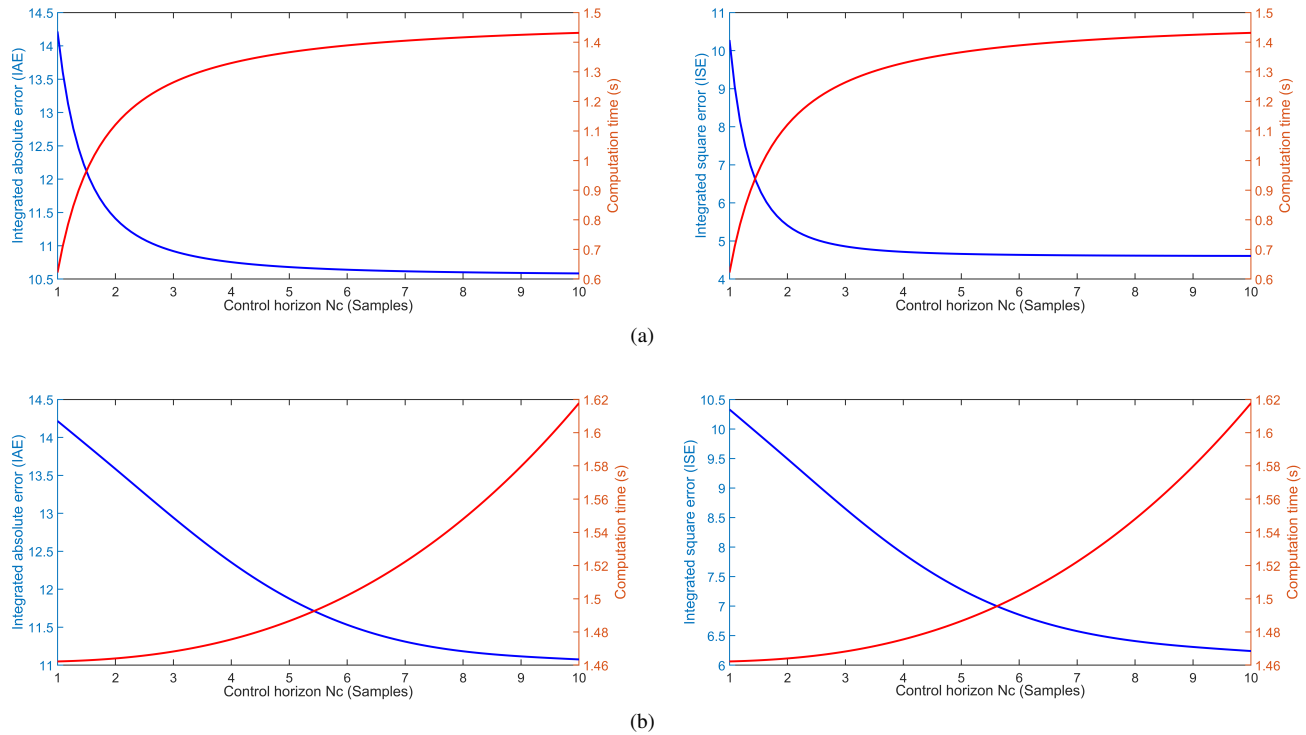$$G_{54}(s) = \frac{-0.00015}{(s+0.0175+0.0179j)(s+0.0175-0.0179j)}$$

FIGURE 9: Computational time, absolute integral error (IAE) and integral squared error (ISE) for different control horizon values (a) MO-MPC (top figures) and (b) MPC (bottom figures).

$$G_{55}(s) = \frac{0.00147}{(s + 0.025 + 0.0654j)(s + 0.025 - 0.0654j)}$$

$$G_{12} = G_{13} = \cdots = G_{53} = 0.$$

The ranges and operating points of the output variables are listed in Table 3.

TABLE 3: Parameters used in steam/water loop operation

Output variables	Operating points	Range	Units
Drum water level	1.79	[1.39-2.19]	m
Exhaust manifold pressure	100.03	[87.03-133.8]	MPa
Deaerator pressure	30	[24.9-43.86]	KPa
Deaerator water level	0.7	[0.489-0.882]	m
Condenser water level	0.5	[0.32-0.63]	m

The rates and amplitudes of the five manipulated inputs are constrained to:

$$\begin{cases} -0.007 \leq \dfrac{du_1}{dt} \leq 0.007 & 0 \leq u_1 \leq 1 \\ -0.01 \leq \dfrac{du_2}{dt} \leq 0.01 & 0 \leq u_2 \leq 1 \\ -0.01 \leq \dfrac{du_3}{dt} \leq 0.01 & 0 \leq u_3 \leq 1 \\ -0.007 \leq \dfrac{du_4}{dt} \leq 0.007 & 0 \leq u_4 \leq 1 \\ -0.007 \leq \dfrac{du_5}{dt} \leq 0.007 & 0 \leq u_5 \leq 1 \end{cases} \quad (14)$$

The input units are normalized as percentage values of the valve opening (i.e., 0 represents a fully closed valve, and

1 is completely opened). Additionally, the input rates are measured in percentage per second.

We compare performance of MO-MPC, distributed MPC and centralized MPC. In particular for this process, a distributed MO-MPC as proposed in [18] is applied to the steam/water loop, in which the outputs of the controller are calculated individually, as through a communication network, the interactions of the system take place. The controller tuning parameters are summarized in Table 4. The tuning of the parameters followed the recommendations from [25].

TABLE 4: Controller Parameters

Con-trol	N_1 Samples	N_2 Samples	N_c Samples	$T_s(s)$	Noise Filter:C/D
Loop1	1	20	1		
Loop2	1	15	1		
Loop3	1	15	1	5	$\frac{C(q^{-1})}{(1-q^{-1})A(q^{-1})}$
Loop4	1	20	1		
Loop5	1	20	1		

The simulation performance of the system for all five loops for reference tracking are shown in Fig. 11 and Fig. 12, depicting controlled and manipulated variables and comparing all three control strategies.

A significant difference has been obtained among the two methods, as the computational time for MO-MPC is 2.8085 seconds, while for distributed MPC is 17.7620 and for centralized MPC is 29.3658 seconds. The indexes about tracking
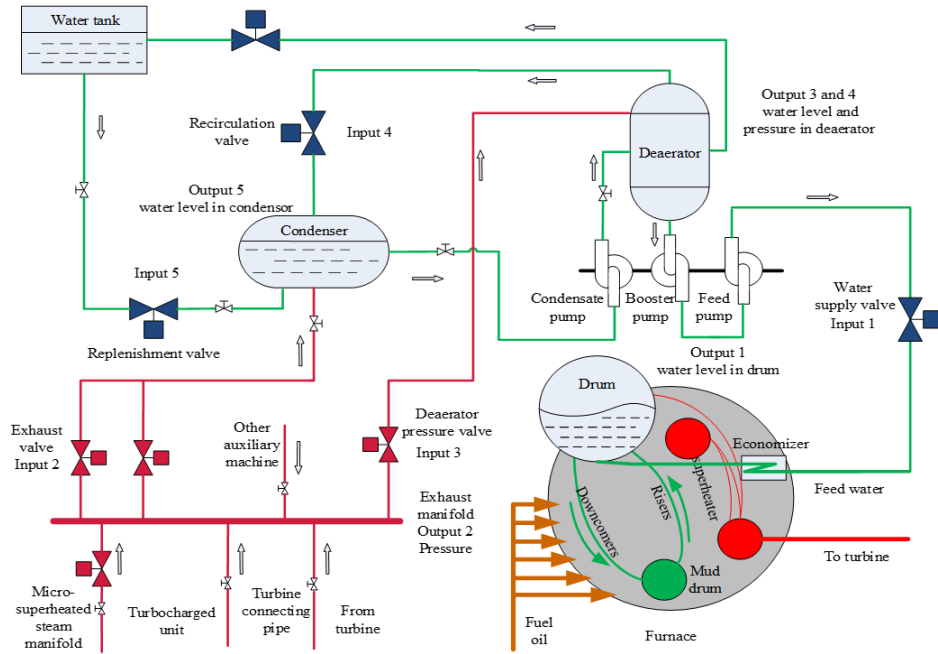
FIGURE 10: Schematic representation of the steam/water loop in large ships and the interaction between the various subsystems; see text for variable notation.

error and control effort are listed in Table 5 with definitions in (15).

$$
\begin{cases}
IARE_i = \sum_{k=0}^{N_S-1} |r_i(k) - y_i(k)| / r_i(k) \ (i = 1, 2, \cdots, 5) \\
ISU_i = \sum_{k=0}^{N_S-1} (u_i(k) - u_{ssi}(k))^2 \ (i = 1, 2, \cdots, 5)
\end{cases}
$$
(15)

The simulation results suggest that a significant computational effort can be saved, without much trade-off for performance and control effort. Despite the high complexity of the interaction in this system, the MO-MPC method proves to be a suitable control strategy.

C. EXAMPLE 3: SEDATION-HEMODYNAMIC REGULATION DURING GENERAL ANESTHESIA

This example is again a relevant choice as discussed in [1], within the biomedical and healthcare systems. The selected process is a regulatory problem for drug management in general anesthesia, with two major systems (counter) interacting in terms of clinical effects: sedation and hemodynamic state. The regulatory paradigm has been detailed in [59], [70]–[72]. The conceptual representation of the various synergic and antagonistic interactions between sedation and hemodynamic systems is given in Fig. 13.

The following is a description of the model parameters and the references from where their values have been extracted or adapted to mimic the clinical effect.

The PK part of the hypnosis model is a transfer function model of the form

$$
H_P(s) = \frac{K(s + z_1)(s + z_2)}{(s + p_1)(s + p_2)(s + p_3)(s + p_4)}
$$
(16)

with parameters $z_1 = -10; z_2 = -15; p_1 = -1; p_2 = -0.8; p_3 = -0.02; p_4 = -0.5$ and $K = -0.005$. The hypnotic drug input of this model is Propofol (mg/kg*min) and the output is effect site concentration CeP (mg/ml). The PD part of the hypnosis model is a nonlinear Hill curve in the form

$$
Effect = \frac{CeP^{\gamma_P}}{CeP^{\gamma_P} + C50P^{\gamma_P}}
$$
(17)

where CeP is the output of the PK model from (16), $C50P$ is the concentration at half-effect and γ_P denotes the drug resistance/sensitivity of the patient. For this simulator, the values $C50P = 2.2$ and $\gamma_P = 2$. The PK part of the analgesia model is a transfer function model of the form as in (16) with parameters $z_1 = -15; z_2 = -5; p_1 = -2; p_2 = -1.5; p_3 = -0.01; p_4 = -0.75$ and $K = -0.0025$. The opioid drug input of this model is Remifentanil (mg/kg*min) and the output is effect site concentration CeR (mg/ml). The PD part of the hypnosis model is a nonlinear Hill curve in the form of (17), with values $C50R = 13.7$ and $\gamma_R = 2.4$ have been used. The combined synergic effect of Propofol and Remifentanil on the hypnotic output (Bispectral Index in this case) has been taken into account in a simplified model proposed in [73]. There is evidence to support the claim that Remifentanil affects negatively mean arterial pressure (MAP) and a model has been approximated from [74]:

$$
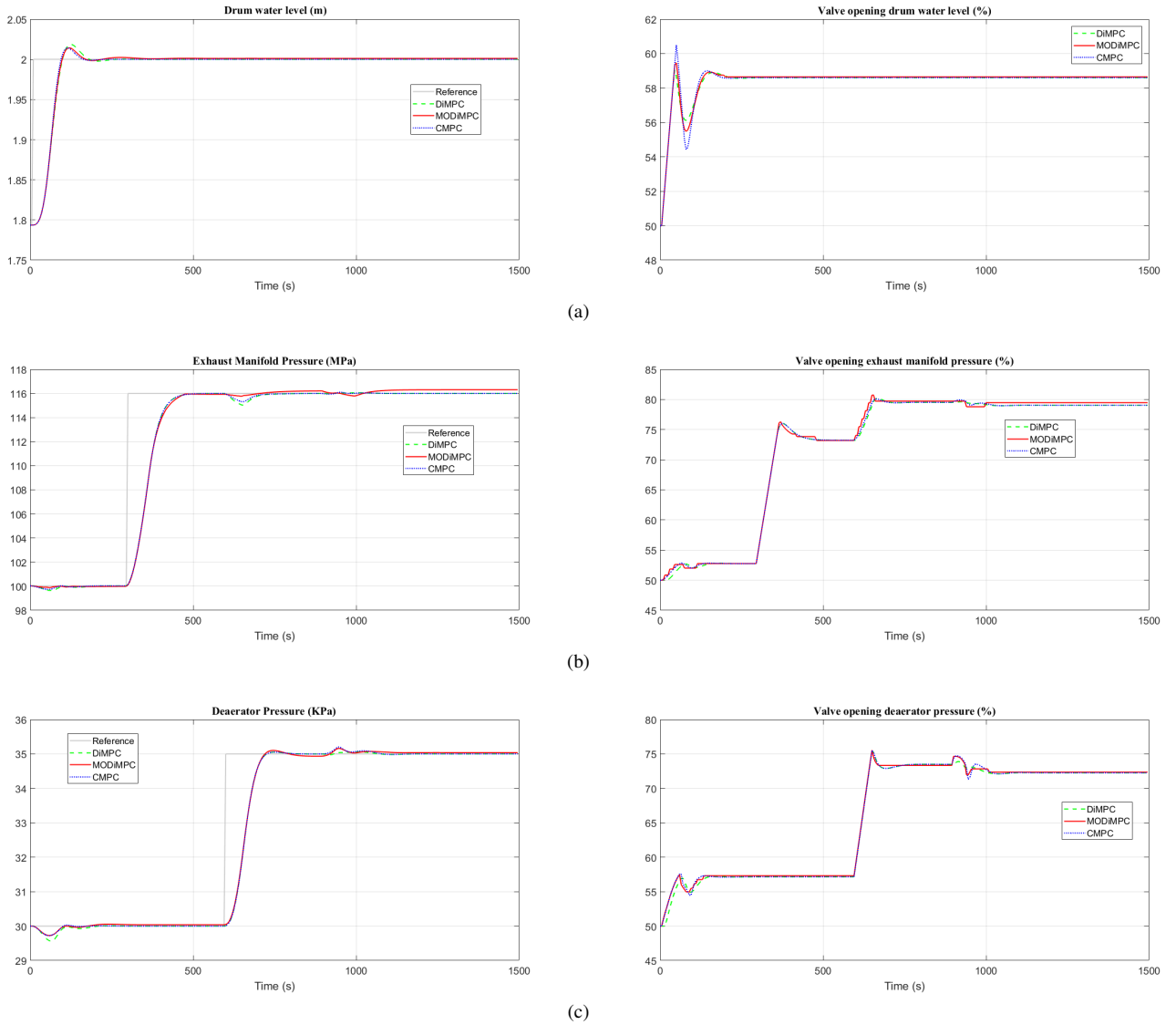MAP_{Remi} = \frac{-1}{0.81 * 15s + 0.81}
$$
(18)

(a)

(b)

(c)

FIGURE 11: Responses of the steam/water loop under the MODIMPC, distributed (DIMPC) and centralized (CMPC) controllers (a) drum water level control loop, (b) exhaust manifold pressure control loop, (c) deaerator pressure control loop. Left column depicts the controlled variables (reference tracking test), right column gives the manipulated variables.

TABLE 5: Performance indexes for the compared controllers

Index	Controller	Loop1	Loop2	Loop3	Loop4	Loop5
IARE	MO-MPC	1.3713	2.1597	2.1788	1.9938	3.6409
	DiMPC	1.0192	1.8132	1.9317	1.5887	3.4300
	MPC	1.1998	1.8919	1.9661	1.8586	3.3456
ISU	MO-MPC	0.0216	0.5152	0.0941	0.1449	1.6413
	DiMPC	0.02412	0.4853	0.09782	0.1492	1.6159
	MPC	0.0237	0.4783	0.0967	0.1413	1.6435

followed by a PD model with $\gamma_{RMAP} = 4.5$ and $C50_{RMAP} = 17$.

The hemodynamic model has been taken from [75] and has two inputs: Dopamine and Sodium Nitroprusside (SNP), and two outputs: Cardiac Output (CO) and MAP:

$$\begin{bmatrix} \frac{5}{300s+1}e^{-60s} & \frac{12}{150s+1}e^{-50s} \\ \frac{3}{40s+1}e^{-60s} & \frac{-15}{40s+1}e^{-50s} \end{bmatrix} \quad (19)$$

This sub-process is a highly challenging one in terms of control, as the time delay is significantly high over the time constant of the process and the system has a large interaction degree. As the cardiac output tends to increase, the hypnotic state tends to increase towards consciousness values, as the drug is cleared at faster rates from the organisms. This antagonistic situation is difficult to maintain in clinical onset.
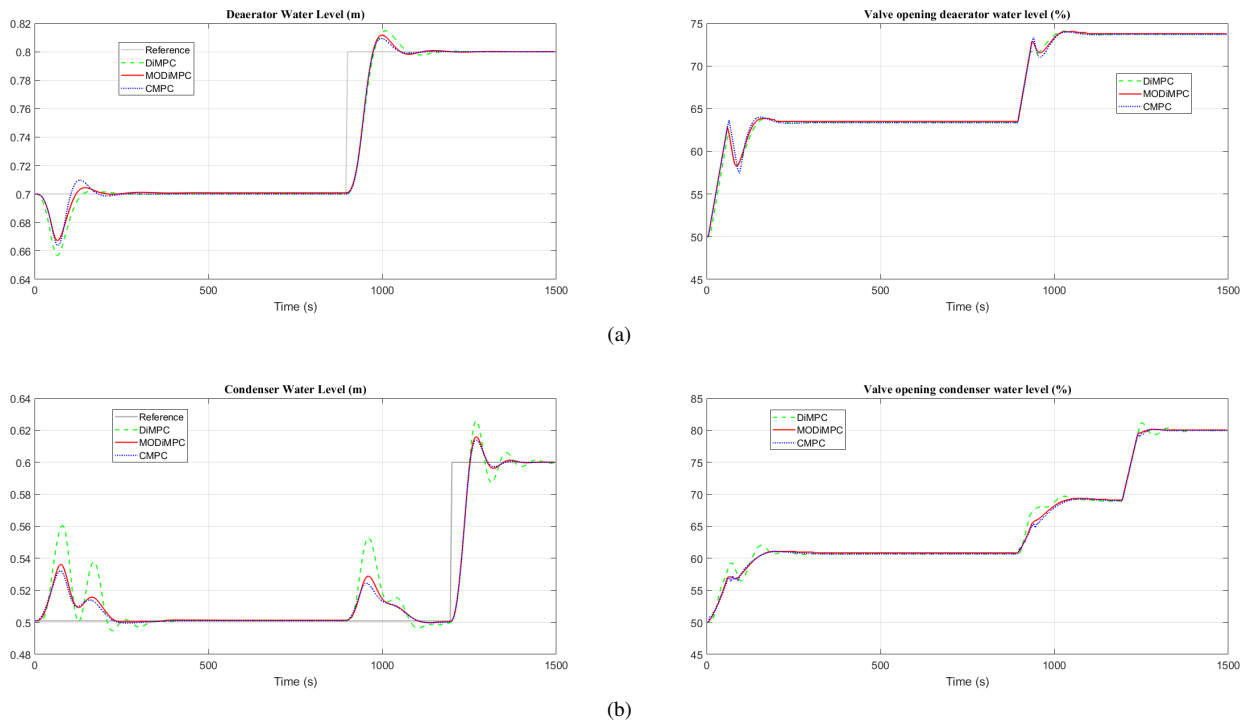
FIGURE 12: Responses of the steam/water loop the MODIMPC, distributed (DIMPC) and centralized (CMPC) controllers (a) deaerator water level control loop and (b) condenser water level control loop. Left column depicts the controlled variables (reference tracking test), right column gives the manipulated variables.

Sedation tends to lower MAP and CO, while these need to be maintained at a safe interval value for the patient to remain in stable vital conditions. The controller parameters for both cases have been a control horizon $N_c = 1$, delay $N_1 = 1$ and prediction horizon of $N_2 = 20$ samples, with a sampling period of 5 seconds. The special scheme for delay compensation has been used as explained in previous section to accommodate the delay values in the hemodynamic model. The results of the comparison are given in Fig. 14 for the sedation state of the patient and in Fig. 15 for the cardiac output. The results indicate the MO-MPC scheme has lower performance compared to the MPC scheme, but manages to remain within the desired tolerance intervals. The computational time for MO-MPC was 1.459 seconds, while for centralized MPC was 2.78 seconds and for distributed MPC was 2.09 seconds.

III. DISCUSSION

The simplified multi-objective approach for optimization of MPC for multivariable systems presented in this paper has the benefit of low computational burden and a relatively easy to implement flow of execution. The results obtained in simulations of representative CPS suggest the method is suitable for control of highly interactive systems with constraints. As safety is taken into account, it implies a minimal stability present in the loop and this is observable from the results. The study has been performed under ideal process dynamic conditions, i.e. no modelling errors were assumed.

In this way, the differences observed between MO-MPC and distributed and centralized MPC algorithms are solely due to the differences in the implementation of the optimization flow diagrams. Analysis in presence of higher model mismatch indicates a performance degradation for MO-MPC, as expected.

The proposed sequential minimal MO-MPC method is applicable to processes which do not require precision control or high control accuracy. Such processes are mainly observed in mechanical system manufacturing and mechatronic applications, and heterogeneous processes such as cyber physical systems. Moreover, process control for product manufacturing, steel, chemical, food and other such related industrial applications always indicates tolerance intervals for performance specifications and requires that most importantly, safety limits are kept at all times. Energy saving by means of penalizing control action variability is an important feature but in this study has been used with lowest priority; we have presented a separate study on a windmill park for indicating the further potential of using multiobjective optimization with various timelapse priorities [29]. One may consider to switch priorities between performance (i.e. product specification) and consumption (i.e. control effort saving). In this case, the MO-MPC results in a conservative performance, i.e. a robust control which may be relevant in case of high model-plant mis-match.

Finally, from all relevant features of CPS we have successfully addressed most of them, in what concerns hetero-
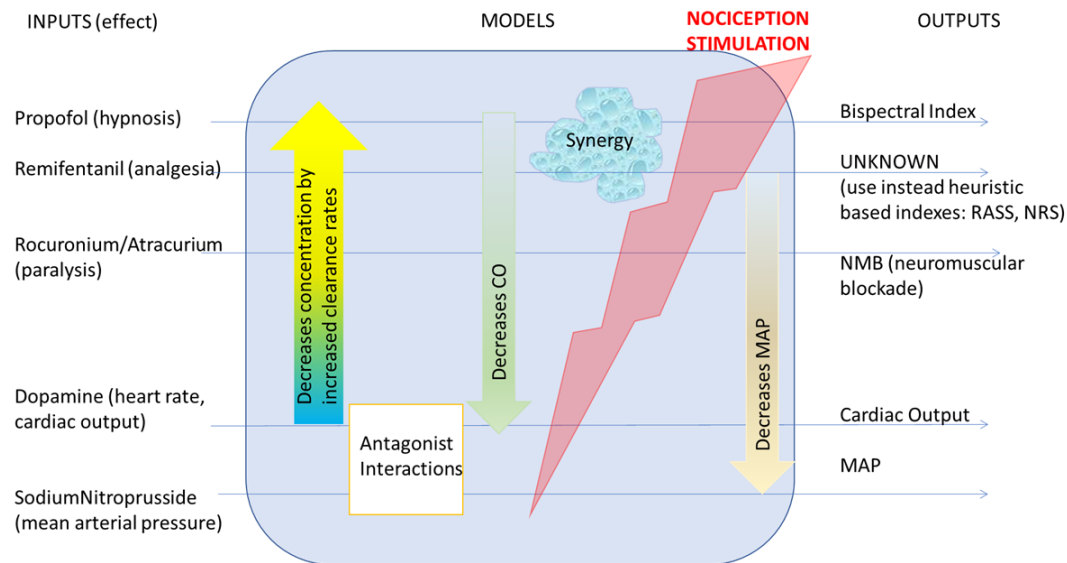
IEEE *Access*

FIGURE 13: Conceptual representation of the interactions present in the sedation and hemodynamic systems during general anesthesia.
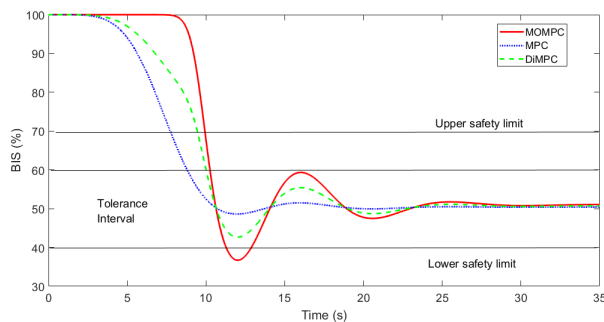

FIGURE 14: Hypnosis induction phase for MO-MPC, MPC and DIMPC optimization schemes.
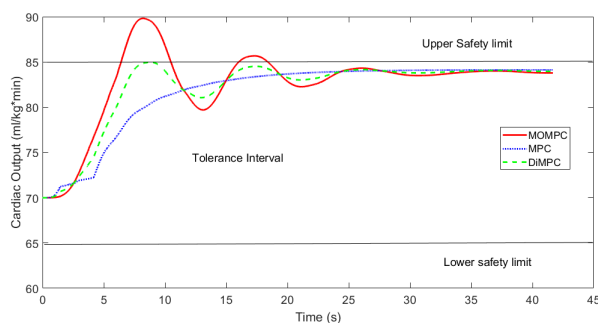

FIGURE 15: Cardiac output regulation during the induction phase for MO-MPC, MPC and DIMPC optimization schemes.

geneity of the sub-systems, strong interactions, distributed control and multi-objective optimization requirements. The examples presented in this paper are versatile and may be used as a basis for other related applications.

As a further challenge related to CPS, it would be interesting to investigate the effect of variable time delays with the proposed scheme against a fully compensated centralized MPC scheme.

REFERENCES

[1] R. Baheti and H. Gill, "Cyber-physical systems," *The Impact of Control Technology, (Eds) T. Samad and A. Annaswamy*, p. 6, 2011.
[2] C. Lv, Y. Liu, X. Hu, H. Guo, D. Cao, and F. Wang, "Simultaneous observation of hybrid states for cyber-physical systems: A case study of electric vehicle powertrain," *IEEE Transactions on Cybernetics*, vol. 48, no. 8, pp. 2357–2367, Aug 2018.
[3] C. Lv, Y. Xing, J. Zhang, X. Na, Y. Li, T. Liu, D. Cao, and F. Wang, "Levenberg–marquardt backpropagation training of multilayer neural networks for state estimation of a safety-critical cyber-physical system," *IEEE Transactions on Industrial Informatics*, vol. 14, no. 8, pp. 3436–3446, Aug 2018.
[4] R. Vaiana, T. Luele, V. Astarita, M. Caruso, A. Tassitani, C. Zaffino, and V. Giofre, "Driving behavior and traffic safety: An acceleration-based safety evaluation procedure for smartphones," *Modern Applied Science*, vol. 8, no. 1, pp. 88–96, Jan 2014.
[5] G. Li, F. Zhu, X. Qu, B. Cheng, S. Li, and P. Green, "Driving style classification based on driving operational pictures," *IEEE Access*, vol. 7, pp. 90 180–90 189, 2019.
[6] M. Bauer, A. Horch, L. Xie, M. Jelali, and N. Thornhill, "The current state of control loop performance monitoring - a survey of application in industry," *Journal of Process Control*, vol. 38, no. -, pp. 1–10, 2016.
[7] A. Maxim, D. Copot, C. Copot, and C. Ionescu, "The 5Ws for control as part of industry 4.0: why, what, where, who, and when - a PID and MPC control perspective," *Inventions*, vol. 4, no. 11, 2019.
[8] T. Samad, "A survey on industry impact and challenges thereof," *IEEE Ctrl Syst Mag*, vol. 37, no. 1, pp. 17–18, 2017.
[9] K. Starr, *Single loop control methods*. Sweden: ABB Inc., 2015.

[10] S. Qin and T. Badgwell, "A survey of industrial model predictive control technology," *Control Engineering Practice*, vol. 11, pp. 733–764, 2003.

[11] T. Badgwell and S. Qin, "Model-predictive control in practice," *Encyclopedia of Systems and Control*, vol. Springer Verlag London, 2014.

[12] M. Morari and J. Lee, "Model predictive control: past, present and future," *Computers and Chemical Engineering*, vol. 23, no. 4–5, pp. 667–682, 1999.

[13] C. Garcia, D. Prett, and M. Morari, "Model predictive control: theory and practice - a survey," *Automatica*, vol. 25, no. 3, pp. 335–348, 1989.

[14] R. Findeisen, L. Imsland, and F. Allg "State and output feedback nonlinear model predictive control: an overview," *European Journal of Control*, vol. 9, no. 2-3, pp. 190–206, 2003.

[15] A. Rossiter, *Model Predictive Control: a practical approach*. CRC Press, 2003.

[16] E. Camacho and C. Bordons, *Model Predictive Control*. Springer Verlag London, 2005, 2nd edition.

[17] D. Fu, C. Ionescu, E. Aaghezzaf, and R. De Keyser, "Decentralized and centralized model predictive control to reduce the bullwhip effect in supply chain management," *Computers and Industrial Engineering*, vol. 73, pp. 21–31, 2014.

[18] A. Maxim, D. Copot, R. De Keyser, and C. Ionescu, "An industrially relevant formulation of a distributed model predictive control algorithm based on minimal process information," *Journal of Process Control*, vol. 68, no. -, pp. 240–253, 2018.

[19] D. Fu, H. Zhang, Y. Yu, C. Ionescu, E.-H. Aghezzaf, and R. De Keyser, "A distributed model predictive control strategy for the bullwhip reducing inventory management policy," *IEEE Trans Ind Inf*, vol. 15, no. 2, pp. 932–941, 2019.

[20] X. Kong, X. liu, L. Ma, and K. Lee, "Hierarchical distributed model predictive control of standalone wind/solar/battery power systems," *IEEE Trans Syst Man Cyber: Systems*, vol. 49, no. 8, pp. 1570–1581, 2019.

[21] R. De Keyser and A. Van Cauwenberghe, "A self-tuning predictor as operator guide," *In: R. Isermann (Ed.), Identification and System Parameter Estimation*, pp. 1249–1256, 1979.

[22] M. Forbes, R. Patwardhan, H. Hamadah, and R. Gopaluni, "Model predictive control in industry: challenges and opportunities," in *IFAC papersOnline 48-8*. IFAC, 2015, 531–538.

[23] W. Wojsznis, J. Gudaz, T. Blevins, and A. Mehta, "Practical approach to tuning MPC," *ISA Transactions*, vol. 42, no. -, pp. 149–162, 2003.

[24] J. Richalet and D. O'Donovan, *Predictive functional control*. Springer-Verlag, London: Springer, 2009.

[25] C. Ionescu and D. Copot, "Hands-on MPC tuning for industrial applications," *Bulletin of the Polish Academy of Sciences: Technical Sciences*, vol. 67, no. 5, pp. 925–945, 2019.

[26] D. He, L. Wang, and J. Sun, "On stability of multiobjective nmpc with objective prioritization," *Automatica*, vol. 57, pp. 189–198, 2015.

[27] D. He, L. Wang, and L. Yu, "Multi-objective nonlinear predictive control of process systems: a dual-mode tracking control approach," *Journal of Process Control*, vol. 25, pp. 142–151, 2015.

[28] K. Lesser and A. Abate, "Multi-objective optimal control with safety as a priority," in *2017 Int Conf on Cyber Physical Systems*. Pittsburgh, PA, USA, April: ACM, 2017, 25–36.

[29] C. Ionescu, C. F. Caruntu, R. Cajo, M. Ghita, G. Crevecoeur, and C. Copot, "Multi-objective predictive control optimization with varying term objectives: a windfarm case study," *Processes*, vol. 7(778), no. 778, 2019.

[30] J. Lu, R. Zhang, K. Yao, and F. Gao, "A multi-objective model predictive control for temperature control in extrusion processes," in *2017 6th Int Symp on Advanced Control of Industrial Processes (AdCONIP)*. Taipei, Taiwan, May 28-31: IEEE, 2017, 31–36.

[31] W. Wojsznis, A. Mehta, P. Wojsznis, D. Thiele, and T. Blevins, "Multi-objective optimization for model predictive control," *ISA Transactions*, vol. 46, pp. 351–361, 2007.

[32] J. Maree and L. Imsland, "On multi-objective economic predictive control for cyclic process operation," *Journal of Process Control*, vol. 24, pp. 1328–1336, 2014.

[33] A. Nunez, C. Cortes, D. Saez, B. De Schutter, and M. Gendreau, "Multi-objective model predictive control for dynamic pickup and delivery problems," *Control Engineering Problems*, vol. 32, pp. 73–86, 2014.

[34] M. Li, P. Zhou, H. Wang, and T. Chai, "Nonlinear multi-objective MPC-based optimal operation of a high consistency refining system in papermaking," *IEEE Trans Syst Man Cyber: Systems*, p. early access: 8, 2017.

[35] X. Zeng, Z. Liu, and Q. Hui, "Energy equipartition stabilization and cascading resilience optimization for geospatially distributed cyber-physical

network systems," *IEEE Transactions on Systems, Man, and Cybernetics: Systems*, vol. 45, no. 1, pp. 25–43, Jan 2015.

[36] J. Tavčar and I. Horváth, "A review of the principles of designing smart cyber-physical systems for run-time adaptation: Learned lessons and open issues," *IEEE Transactions on Systems, Man, and Cybernetics: Systems*, vol. 49, no. 1, pp. 145–158, Jan 2019.

[37] J. Cecil, S. Albuhamood, A. Cecil-Xavier, and P. Ramanathan, "An advanced cyber physical framework for micro devices assembly," *IEEE Transactions on Systems, Man, and Cybernetics: Systems*, vol. 49, no. 1, pp. 92–106, Jan 2019.

[38] R. De Keyser and A. Van Cauwenberghe, "A self-tuning multistep predictor application," *Automatica*, vol. 17, no. 1, pp. 167–174, 1981.

[39] R. De Keyser, "Model based predictive control for linear systems," *UN-ESCO Encyclopaedia of Life Support Systems, Control Systems, Robotics and Automation*, vol. Vol. XI, Article contribution 6.43.16.1, Eolss Publishers Co Ltd, Oxford, no. -, p. 30 pages, 2003.

[40] N. Nicolai, F. De Leersnyder, D. Copot, M. Stock, C. Ionescu, K. Gernaey, I. Nopens, and T. De Beer, "Liquid-to-solid ratio control as an advanced process control solution for continuous twin-screw wet granulation," *AICHE Journal*, vol. 64, pp. 2500–2514, 2018.

[41] A. Dutta, *Design and Certification of Industrial Predictive Controllers*. Ghent, Belgium: Doctoral Thesis Academic Press, Ghent University, 2015.

[42] A. Dutta, J. Maciejowski, E. Hartley, and R. De Keyser, "Certification of a class of industrial predictive controllers without terminal conditions," in *2014 53rd IEEE Annual Conference on Decision and Control (CDC)*. Los Angeles, CA, USA, December 15-17: IEEE, 2014, 6695–6700.

[43] J. Castano, A. Hernandez, Z. Li, N. Tsagarakis, and R. De Keyser, "Enhancing the robustness of the epsac predictive control using singular value decomposition approach," *Robotics and Autonomous Systems*, vol. 74, pp. 283–295, 2015.

[44] C. Muresan, C. Ionescu, E. Dulf, R. Rusu-Both, and S. Folea, "Advantage of low cost predictive control: study case on a train of distillation columns," *Chemical Engineering and Technology*, vol. 41, no. 10, pp. 1936–1948, 2018.

[45] B. Huyck, J. De Brabanter, B. De Moor, J. Van Impe, and F. Logist, "Online model predictive control of industrial processes using low level control hardware: a pilot scale distillation column case study," *Control Engineering Practice*, vol. 28, no. -, pp. 34–48, 2014.

[46] R. De Keyser and C. Ionescu, "Minimal information based simple identification method of fractional order systems for model based control applications," in *11th Asian Control Conference*. Gold Coast, December 17–20, Australia: IEEE, 2017, 1411–1416.

[47] R. De Keyser and C. Ionescu, "The disturbance model in model based predictive control," in *IEEE Conf on Control Applications*. Istanbul, June 23-25, Turkey: IEEE, 2013, 446–451.

[48] Y. Song, Z. Wang, S. Liu, and G. Wei, "N-step MPC for systems with persistent bounded disrtubances under SCP," *IEEE Trans Syst Man Cyber: Systems*, p. early access: 11, 2018.

[49] A. Bemporad and D. de la Pena, "Multi-objective model predictive control," *Automatica*, vol. 45, pp. 2823–2830, 2009.

[50] A. Yamashita, A. Zanin, and D. Odloak, "Tuning of model predictive control with multi-objective optimization," *Brazilian Journal of Chemical Engineering*, vol. 33, no. 2, pp. 333–346, 2016.

[51] K. Tan, E. Khor, T. Lee, and R. Sathikannan, "An evolutionary algorithm with advanced goal and priority specification for multi-objective optimization," *Journal of Artificial Intelligence Research*, vol. 18, pp. 183–215, 2003.

[52] Y. Fend, M. Zhou, G. Tian, Z. Li, Z. Zhang, Q. Zhang, and J. Tan, "Target disassembly sequencing and scheme evaluation for CNC machine tools using improved multi-objective ant colony algorithm and fuzzy integral," *IEEE Trans Syst Man Cyber: Systems*, vol. 49, no. 12, pp. 2438 – 2451, 2019.

[53] Z. Zhang, S. Chen, J. Xie, and S. Yang, "Two hybrid multi-objective motion planning schemes synthesized by recurrent neural networks for wheeled mobile robot manipulators," *IEEE Trans Syst Man Cyber: Systems*, p. early access: 12, 2019.

[54] W. Lakhdhar, R. Mzid, M. Khalgui, Z. Li, G. Frey, and A. Al-Ahmari, "Multi-objective optimization approach for a portable development of reconfigurable real-time systems: from specification to implementation," *IEEE Trans Syst Man Cyber: Systems*, vol. 49, no. 3, pp. 623–637, 2019.

[55] B. Alagoz, G. Kavuran, A. Ates, and C. Yeroglu, "Reference-shaping adaptive control by using gradient descent optimizers," *PLoS One*, vol. 12, no. 11, p. e0188527, 2017.

This article has been accepted for publication in a future issue of this journal, but has not been fully edited. Content may change prior to final publication. Citation information: DOI 10.1109/ACCESS.2020.3007924, IEEE Access

Ionescu *et al.*: Multi-objective optimization procedure for predictive control towards cyber physical systems

[56] B. Alagoz, A. Tepljakov, G. Kavuran, and H. Alisoy, "Adaptive control of nonlinear TRMS model by using gradient descent optimizers," in *Int Conf on Artificial Intelligence and Data Processing*. IEEE, 2018.

[57] C. Ionescu, C. Muresan, D. Copot, and R. De Keyser, "Constrained multivariable predictive control of a train of cryogenic 13C separation columns," in *11th IFAC Symposium on Dynamics and Control of Process Systems*. Trondheim, June 6–8, Norway: IFAC, 2016, 1103–1108.

[58] M. Sbarciog, R. De Keyser, S. Cristea, and C. De Prada, "Nonlinear predictive control of processes with variable time delay. a temperature control case study," in *IEEE International Conference on Control Applications*. San Antonio, CA Date: SEP 03-05: IEEE, 2008, 601–606.

[59] C. Ionescu, R. Hodrea, and R. De Keyser, "Variable time-delay estimation for anesthesia control during intensive care," *IEEE Transactions on Biomedical Engineering*, vol. 58, pp. 363–369, 2011.

[60] J. Normey-Rico, *Control of Dead-Time processes*. London: Springer, 2007.

[61] C. Pop, C. Ionescu, and R. De Keyser, "Time delay compensation for the secondary processes in a multivariable carbon isotope separation unit," *Chemical Engineering Science*, vol. 80, no. -, pp. 205–218, 2012.

[62] P. Van de Voorde, S. Gautama, A. Momont, C. Ionescu, P. De Paepe, and N. Freyman, "The drone ambulance [a-uas]: golden bullet or just a blank?" *Resuscitation*, vol. 116, pp. 46–48, 2017.

[63] R. Cajo, T. M. Thi, C. Copot, D. Plaza, R. De Keyser, and C. Ionescu, "Multiple UAVs formation for emergency equipment and medicines delivery based on optimal fractional order controllers," in *2019 IEEE International Conference on Systems, Man and Cybernetics (SMC)*, Oct 2019, pp. 318–323.

[64] A. Hernandez, H. Murcia, C. copot, and R. De Keyser, "Towards the development of a smart flying sensor: illustration in the field of precision agriculture," *Sensors*, vol. 15, no. 7, pp. 16 688–16 709, 2015.

[65] P. Bristeau, F. Callou, D. Vissiere, and N. Petit, "The navigation and control technology inside the ar.drone micro uav," *IFAC Proceedings Volumes*, vol. 44, no. 1, pp. 1477–1484, 2011.

[66] T. T. Mac, C. Copot, A. Hernandez, and R. De Keyser, "Improved potential field method for unknown obstacle avoidance using uav in indoor environment," in *2016 IEEE 14th International Symposium on Applied Machine Intelligence and Informatics (SAMI)*. HerLany, Slovakia, 20-22 January: IEEE, 2016, 345–350.

[67] T. Mac, C. Copot, R. De Keyser, and C. M. Ionescu, "The development of an autonomous navigation system with optimal control of an uav in partly unknown indoor environment," *Mechatronics*, vol. 49, pp. 187 – 196, 2018.

[68] S. Zhao, A. Maxim, L. Sheng, R. De Keyser, and C. M. Ionescu, "Effect of control horizon in model predictive control for steam/water loop in large-scale ships," *Processes (open access)*, vol. 6, no. 12, 2018.

[69] S. Zhao, R. Cajo, R. De Keyser, S. Liu, and C. Ionescu, "Nonlinear predictive control applied to steam/water loop in large scale ships," in *2019 12th IFAC Symposium on Dynamics and Control of Process Systems, including Biosystems*. Florianopolis, Brazil, 23-26 April: IFAC, 2019, 868–873.

[70] C. Ionescu, R. De Keyser, B. Torrico, T. De Smet, M. Struys, and J. Normey-Rico, "Robust predictive control strategy applied for propofol dosing using BIS as a controlled variable," *IEEE Transactions on Biomedical Engineering*, vol. 55, pp. 2161–2170, 2008.

[71] C. Ionescu, D. Copot, M. Neckebroek, and C. Muresan, "Anesthesia regulation: towards completing the picture," in *21st IEEE International Conference on Automation, Quality and Testing, Robotics (AQTR THETA)*. Cluj-Napoca, Romania, 24-26 May: IEEE, 2018, -.

[72] C. Ionescu and D. Copot, "Drug delivery system for general anesthesia: Where are we?" in *IEEE International Conference on Systems Man and Cybernetics Conference Proceedings*. San Diego, USA, 05–08 October: IEEE, 2014, 2452–2457.

[73] C. Ionescu, "A computationally efficient Hill curve adaptation strategy during continuous monitoring of dose-effect relation in anesthesia," *Nonlinear Dynamics*, vol. 92, no. 3, pp. 843–852, 2018.

[74] J. Standing, G. Hammer, and D. Drover, "Pharmacokinetic-pharmacodynamics modelling of the hypotensive effect of remifentanil in infants," *Pediatric Anesth*, vol. –, 2009.

[75] C. Palerm and W. Bequette, "Hemodynamic control using direct model reference adaptive control - experimental results," *European J of Control*, vol. 11, pp. 558–571, 2005.

CLARA IONESCU (S'06-M'08-S'19) received the M.Sc. degree in industrial informatics and automation from the Dunarea de Jos University of Galati, Romania, in 2003, and the Ph.D. degree from Ghent University, Belgium, in 2009 on modelling the human respiratory system with fractional order models for diagnosis purposes. Between 2011-2016 she was the recipient of the prestigious Flanders Research Fund grant for post-doctoral fellows at the same university. Since October 2016 she is professor at Ghent University, teaching Computer Control of Industrial Processes within the Control and Automation Master Program. She is working on the application of generic control algorithms (fractional, predictive and PID-type) to dynamic processes in various application fields.

RICARDO ALFREDO CAJO DIAZ received the B.Eng. degree in telecommunications engineering and his M.Sc. degree in industrial automatic control from the Escuela Superior Politécnica del Litoral (ESPOL) in Guayaquil, Ecuador. He is currently a Ph.D. Researcher with the Dynamical Systems and Control research group at Ghent University, Belgium. His topics of research are focused on fractional order control, identification and optimization control for fleeting autonomous vehicles.

SHIQUAN ZHAO received the B.S. degree in Electrical Engineering and Automation from Harbin Engineering University, Harbin, China, in 2013 and Master degree in 2018 from the same university. He was recipient of Chinese Scholarship Council for visiting the Dynamical Systems and Control research laboratory in Ghent Univeristy, Belgium. He is currently pursuing the Ph.D. degree at same university. His main research interests include the control strategy of steam power plant, sliding mode control, model predictive control and PID auto-tuning methods.

MIHAELA GHITA received the M.Sc. degree in medical informatics from the Politechnica University in Bucharest, Romania in 2018. The research related to her Master Thesis work was awarded Best Paper Young Author Award at 2019 IEEE-SAMI conference in Herlany, Slovakia. Currently, she is recipient of the prestigious Phd scholarship from Flanders Research Foundation, Belgium and pursuing the PhD degree at Ghent University, Belgium. Her research interest is on modelling and control of drug delivery systems.

MARIA GHITA received the M.Sc. degree in medical informatics from the Politechnica University in Bucharest, Romania in 2018, and her work was awarded the 2018 IEEE Systems Man and Cybernetics MSc Thesis Grant Initiative for the contributions on non-invasive and objective pain level assessment methods. She is recipient of the doctoral scholarship from Special Research Funds of Ghent University, Belgium. Her research interests are on modelling biological tissues and developing optimal control therapies for fighting cancer.

DANA COPOT received the M.Sc. degree in chemical engineering from the Gh. Asachi Politechnica University in Iasi, Romania in 2012. She obtained her PhD degree at Ghent University in 2018 on modelling diffusion mechanisms in biological tissues. Currently she is the recipient of the prestigious Flanders Research Foundation grant for post-doctoral fellows at the same university. Her main research topic is predictive control of drug delivery systems.

• • •